Artificial Equilibrium Points for an Electric Sail with Constant Attitude

Generoso Aliasi* Giovanni Mengali† and Alessandro A. Quarta‡

University of Pisa, I-56122 Pisa, Italy

Introduction

Creating and maintaining Artificial Equilibrium Points (AEPs) in the restricted three-body problem is a challenging mission scenario in which a propellantless propulsion system exploits its natural potential [1]. Indeed, in such a problem the acceleration resulting from the sum of centrifugal and gravitational forces can be balanced, for a theoretically unlimited time period, by means of a suitable continuous propulsive thrust.

A thorough analysis involving the location and stability of AEPs has been addressed in a recent paper [2], under the assumption that the propulsion system provides a purely radial thrust with respect to the Sun, and the thrust modulus is a function of the Sun-spacecraft distance only . In that way, with a unified mathematical model, it is possible to analyze the performance of different propulsion systems, as, for example, a photonic solar sail and an Electric Solar Wind Sail (E-Sail). In particular, an E-Sail is known to be able to provide a continuous propulsive acceleration by means of Coulomb's interaction of a number of positively charged tethers with the solar wind plasma stream [3].

As long as the propulsive acceleration is assumed to be radial, as per Ref. [2], the E-sail nominal plane is orthogonal to the Sun-spacecraft direction. However, in a more general case,

*Ph.D. Candidate, Department of Civil and Industrial Engineering, g.aliasi@dia.unipi.it.

†Professor, Department of Civil and Industrial Engineering, g.mengali@ing.unipi.it. Senior Member AIAA.

‡Associate Professor, Department of Civil and Industrial Engineering, a.quarta@ing.unipi.it. Associate Fellow AIAA.

the spacecraft propulsive acceleration direction may be inclined (within prescribed limits) with respect to the radial direction, and a transverse thrust component may be generated. The latter, in its turn, introduces an additional degree of freedom that can be exploited to expand the region of admissible AEPs. The study of such a region for an E-Sail based spacecraft is the subject of this Note, whose aim is to extend the result of Ref. [2] by removing the assumption of radial direction for the propulsive acceleration. Moreover this work, dealing with E-Sails, complements the analysis of Baoyin and McInnes [4], which refers to photonic solar sails.

More precisely, to reduce the active attitude control effort, the E-Sail nominal plane is here assumed to maintain a constant orientation in an orbital reference frame, and the problem of calculating the maps of AEPs position as a function of the E-sail attitude and performance is addressed within an elliptical restricted three-body problem. A linear stability analysis of AEPs near the Lagrange points L_1 and L_4 in the Sun-[Earth+Moon] system is finally discussed, with the aid of Floquet's theory.

Equations of Motion

Consider the motion of a spacecraft equipped with an E-Sail propulsion system, under the gravitational effects of the Sun and a Planet with masses $m_\odot$ and m_P, respectively. The two celestial bodies cover elliptic orbits around their center-of-mass C, and the time-dependent distance between the two celestial bodies [5] is $\ell = a\,(1-e^2)\,g$, with

$$g \triangleq \frac{1}{1+e\cos\nu} \tag{1}$$

where ν, a and e are true anomaly, semi-major axis and eccentricity of the Planet's orbit, see Fig. 1 . Let $\mathcal{T}(C;x,y,z)$ be a non-uniformly rotating (synodic) reference frame with unit vectors $\hat{\boldsymbol{\imath}}$, $\hat{\boldsymbol{\jmath}}$ and $\hat{\boldsymbol{k}}$, whose z axis is in the direction of the Planet's angular momentum,

$\hat{\boldsymbol{\imath}}$ points toward the Planet at any time instant, and $\hat{\boldsymbol{\jmath}} \triangleq \hat{\boldsymbol{\imath}} \times \hat{\boldsymbol{k}}$. The angular velocity of the synodic reference frame with respect to an inertial reference frame is $\boldsymbol{\omega} = \omega\,\hat{\boldsymbol{k}}$, where $\omega = \sqrt{a\,(1-e^2)\,G\,(m_\odot + m_P)}/\ell^2$ and G is the universal gravitational constant. According to Szebehely [5] , the spacecraft vectorial equation of motion in the synodic reference frame may be written as

$$\frac{\mathrm{d}^2(\ell\,\boldsymbol{r})}{\mathrm{d}t^2} + 2\,\boldsymbol{\omega} \times \frac{\mathrm{d}(\ell\,\boldsymbol{r})}{\mathrm{d}t} + \ell\,\frac{\mathrm{d}\boldsymbol{\omega}}{\mathrm{d}t} \times \boldsymbol{r} + \ell\,\boldsymbol{\omega} \times (\boldsymbol{\omega} \times \boldsymbol{r}) = -\frac{G\,m_\odot}{\ell^2\,\rho_\odot^3}\,\boldsymbol{\rho}_\odot - \frac{G\,m_P}{\ell^2\,\rho_P^3}\,\boldsymbol{\rho}_P + \boldsymbol{a}_p \qquad (2)$$

where $\mu \triangleq m_P/(m_\odot + m_P)$ is the dimensionless mass of the Planet, $\boldsymbol{a}_p$ is the propulsive acceleration vector , $\boldsymbol{\rho}_\odot = \boldsymbol{r} + \mu\,\hat{\boldsymbol{\imath}}$, $\boldsymbol{\rho}_P = \boldsymbol{r} - (1-\mu)\,\hat{\boldsymbol{\imath}}$, and $\boldsymbol{r}$ (with $\rho_\odot \triangleq \left\|\boldsymbol{\rho}_\odot\right\|$ and $\rho_P \triangleq \|\boldsymbol{\rho}_P\|$) represent the dimensionless position vectors of the spacecraft with respect to the Sun, the Planet and C, respectively (see Fig. 1) . The propulsive acceleration vector, for an E-sail based spacecraft [2, 6], is given by

$$\boldsymbol{a}_p = \beta \frac{G\,m_\odot}{a\,\ell\,\rho_\odot}\,\hat{\boldsymbol{a}}_p \qquad \text{with} \qquad \beta \triangleq \frac{a_c}{G\,m_\odot/a^2} \qquad (3)$$

where $\hat{\boldsymbol{a}}_p \triangleq \boldsymbol{a}_p/\left\|\boldsymbol{a}_p\right\|$, and β represents the sail lightness number, that is, the ratio of the modulus of the propulsive acceleration at a distance a from the Sun (referred to as characteristic acceleration a_c) to the gravitational acceleration due to the Sun at the same distance.

The introduction of the variable length ℓ as the unit of distance implies that all the dimensionless vectors are measured in a synodic reference frame, pulsating synchronously to the motion of the Planet around the Sun. This fact has important consequences on the location of AEPs, as will be explained later.

Introduce now a Radial-Transversal -Normal (RTN) reference frame, whose unit vectors

are defined as (see Fig. 1)

$$\hat{\boldsymbol{\rho}}_{\odot} \triangleq \frac{\boldsymbol{\rho}_{\odot}}{\rho_{\odot}} \quad , \quad \hat{\boldsymbol{t}} \triangleq \frac{\hat{\boldsymbol{k}} \times \hat{\boldsymbol{\rho}}_{\odot}}{\left\| \hat{\boldsymbol{k}} \times \hat{\boldsymbol{\rho}}_{\odot} \right\|} \quad , \quad \hat{\boldsymbol{n}} \triangleq \hat{\boldsymbol{\rho}}_{\odot} \times \hat{\boldsymbol{t}} \tag{4}$$

The orientation of the propulsive acceleration vector $\boldsymbol{a}_p$ is defined by means of the cone angle α and the clock angle δ, where α is the angle between $\hat{\boldsymbol{a}}_p$ and $\hat{\boldsymbol{\rho}}_{\odot}$, while δ is the angle between $\hat{\boldsymbol{t}}$ and the projection of $\hat{\boldsymbol{a}}_p$ onto the $(\hat{\boldsymbol{t}}, \hat{\boldsymbol{n}})$-plane. According to Ref. [7], the cone angle is upper constrained to prevent possible mechanical instabilities, and the maximum value of α is estimated to be about $30°$. The thrust vectoring capability of an E-Sail is therefore described by two control variables, namely $\alpha \in [0°, 30°]$ and $\delta \in [0°, 360°]$. In what follows the study of AEPs will be performed under the assumption that the sail cone and clock angles are both maintained constant, that is $\alpha = \overline{\alpha}$ and $\delta = \overline{\delta}$, where the overbar symbol is added to emphasize a constant value. In this case, the direction of $\hat{\boldsymbol{a}}_p$ remains constant with respect to the RTN reference frame, viz.

$$\hat{\boldsymbol{a}}_p = \cos\overline{\alpha}\,\hat{\boldsymbol{\rho}}_{\odot} + \sin\overline{\alpha}\,\left(\cos\overline{\delta}\,\hat{\boldsymbol{t}} + \sin\overline{\delta}\,\hat{\boldsymbol{n}}\right) \tag{5}$$

This corresponds to a generalization of the results discussed in Ref. [2], where the propulsive acceleration was assumed to be always in the radial direction (that is, $\alpha \equiv 0°$).

The vectorial equation of motion (2) can be transformed in dimensionless form [5] using the true anomaly ν as the independent variable

$$\boldsymbol{r}'' + 2\,\hat{\boldsymbol{k}} \times \boldsymbol{r}' = g\,\left[-\boldsymbol{f} + B\,\frac{1-\mu}{\rho_{\odot}}\,\hat{\boldsymbol{a}}_p - e\,\cos\nu\,\left(\boldsymbol{r}\cdot\hat{\boldsymbol{k}}\right)\,\hat{\boldsymbol{k}}\right] \tag{6}$$

where the prime symbol denotes a derivative taken with respect to ν, $\boldsymbol{f}$ is the opposite of

the sum between gravitational and centrifugal accelerations

$$\boldsymbol{f} \triangleq \frac{1-\mu}{\rho_{\odot}^{3}}\,\boldsymbol{\rho}_{\odot} + \frac{\mu}{\rho_{P}^{3}}\,\boldsymbol{\rho}_{P} + \hat{\boldsymbol{k}} \times \left(\hat{\boldsymbol{k}} \times \boldsymbol{r}\right) \tag{7}$$

while $B \geq 0$, referred to as modified sail lightness number [2], is

$$B \triangleq \beta \left(\frac{1-e^{2}}{1+e\,\cos\nu}\right) \tag{8}$$

In the special case in which $e = 0$, corresponding to the circular restricted three-body problem, B coincides with β.

Artificial Equilibrium Points

The positions of the AEPs in the synodic reference frame are obtained, from Eq. (6), by enforcing the stationary conditions $\boldsymbol{r}'' = \boldsymbol{r}' = 0$. Note that a fixed dimensionless vector $\boldsymbol{r}_0$, when seen by an observer in the synodic reference frame, corresponds to the dimensional vector $\ell\,\boldsymbol{r}_0$. Therefore, the stationary conditions $\boldsymbol{r}'' = \boldsymbol{r}' = 0$ describe a segment, of length $2\,a\,e\,\|\boldsymbol{r}_0\|$, parallel to the direction of $\boldsymbol{r}_0$, along which the spacecraft oscillates back and forth with a period $2\,\pi/\omega$.

From Eq. (6), the AEP positions turn out to be the solutions of the vectorial equation

$$B\,\frac{1-\mu}{\rho_{\odot}}\,\hat{\boldsymbol{a}}_{p} - e\,\cos\nu\,\left(\boldsymbol{r}\cdot\hat{\boldsymbol{k}}\right)\,\hat{\boldsymbol{k}} - \boldsymbol{f} = 0 \tag{9}$$

Recalling that, by assumption, the cone and clock angle are maintained constant, Eq. (9) states that AEPs are possible only if the two following conditions are met: 1) $e\,(\boldsymbol{r}\cdot\hat{\boldsymbol{k}}) = 0$, and 2) B is constant. The first condition states that, if $e \neq 0$, any AEP lie in the orbital plane of two attractors and $\hat{\boldsymbol{a}}_{p} = \hat{\boldsymbol{f}} \triangleq \boldsymbol{f}/\,\|\boldsymbol{f}\|$, see Eq. (9). Such a constraint univocally

defines the values of cone and clock angles, $\overline{\alpha} = \alpha_0$ and $\overline{\delta} = \delta_0$, necessary for maintaining an AEP, see Eqs. (5) and (7). In other terms, an AEP is defined through the equations

$$\hat{\boldsymbol{a}}_{p_0} = \hat{\boldsymbol{f}}_0 \qquad , \qquad B_0 = \frac{\rho_{\odot 0}}{1-\mu} \, \| \boldsymbol{f}_0 \| \tag{10}$$

where the subscript 0 means that the corresponding variable is evaluated when $\boldsymbol{r} = \boldsymbol{r}_0$, $\overline{\alpha} = \alpha_0$, and $\overline{\delta} = \delta_0$. In particular, the second of Eqs. (10) states that the modified lightness number B is a constant. Therefore, from Eqs. (3) and (8), the characteristic acceleration a_c is a function of the true anomaly through the relationship

$$a_c = B_0 \, \frac{G \, m_\odot}{a^2} \left(\frac{1 + e \cos \nu}{1 - e^2} \right) \tag{11}$$

with a maximum value $a_{c_{\max}}$ given by

$$a_{c_{\max}} = B_0 \, \frac{G \, m_\odot}{a^2} \left(\frac{1 + e}{1 - e^2} \right) \tag{12}$$

Note that the (dimensionless) maximum variation in characteristic acceleration Δa_c is a function of the eccentricity e only, that is

$$\frac{\Delta a_c}{a_{c_{\max}}} = \frac{2 \, e}{1 + e} \tag{13}$$

From a practical viewpoint, the required variation of a_c for an E-sail based spacecraft can be achieved by means of a suitable adjustment of the tethers' voltage [6]. In the special case of the circular restricted three-body problem ($e = 0$), Eq. (9) does not depend on the true anomaly, and AEPs may exist also outside the orbital plane of the two attractors [2] with a constant value of a_c, see Eq. (11).

AEPs in the Sun-[Earth+Moon] system

Figure 2 shows the propulsive performance required to generate an AEP in a region close to the classical Lagrange point L_1 ($x/\ell = \boldsymbol{r}\cdot\hat{\boldsymbol{\imath}}$ and $y/\ell = \boldsymbol{r}\cdot\hat{\boldsymbol{\jmath}}$) for the Sun-[Earth+Moon] system ($\mu = 3.0404\times10^{-6}$, $e_\oplus = 0.01671022$ and $a_\oplus = 1.00000011\,\mathrm{AU}$). The solid lines represent the isocontour lines of the maximum characteristic acceleration necessary to maintain an AEP, see Eq. (12), and dashed lines correspond to isocontour lines of the (required) sail cone angle α_0. The shaded region highlights the set of AEPs achievable with a sail cone angle $\alpha_0 \leq 30^\circ$. Because the propulsive acceleration direction must belong to the plane of motion of the attractors, the set of admissible values for δ_0 is restricted to be either 0° (when $y/\ell > 0$) or 180° (when $y/\ell < 0$).

Linear Stability Analysis

The linear stability of an AEP is now analyzed by introducing the transformation $\boldsymbol{r} = \boldsymbol{r}_0 + \delta\boldsymbol{r}$, where $\delta\boldsymbol{r}$ represents a perturbation in the spacecraft position vector. The variational equation of motion of an E-Sail based spacecraft, obtained by linearizing Eq. (6) around $\boldsymbol{r}_0$, is

$$\delta\boldsymbol{r}'' = g\boldsymbol{H}^{\mathrm{T}}\cdot\delta\boldsymbol{r} - 2\,\boldsymbol{E}\cdot\delta\boldsymbol{r}' \tag{14}$$

in which $\boldsymbol{E}$ and $\boldsymbol{H}$ are second order tensors defined as

$$\boldsymbol{E}\cdot\boldsymbol{r} = \hat{\boldsymbol{k}}\times\boldsymbol{r} \qquad , \qquad \boldsymbol{H} = \nabla\left[-\boldsymbol{f} + B\,\frac{1-\mu}{\rho_\odot}\,\hat{\boldsymbol{a}}_p - e\,\cos\nu\,\left(\boldsymbol{r}\cdot\hat{\boldsymbol{k}}\right)\,\hat{\boldsymbol{k}}\right]\Bigg|_0 \tag{15}$$

where ∇ is the shorthand notation for a gradient taken with respect to $\boldsymbol{r}$. Note that $\boldsymbol{H}$ is evaluated at the equilibrium condition.

Introducing the state vector $\boldsymbol{\xi} \triangleq \left[\delta\boldsymbol{r}\cdot\hat{\boldsymbol{\imath}},\ \delta\boldsymbol{r}\cdot\hat{\boldsymbol{\jmath}},\ \delta\boldsymbol{r}\cdot\hat{\boldsymbol{k}},\ \delta\boldsymbol{r}'\cdot\hat{\boldsymbol{\imath}},\ \delta\boldsymbol{r}'\cdot\hat{\boldsymbol{\jmath}},\ \delta\boldsymbol{r}'\cdot\hat{\boldsymbol{k}}\right]^{\mathrm{T}}$, the lin-

earized equation of motion takes the compact form

$$\boldsymbol{\xi}' = \mathbb{A}\,\boldsymbol{\xi} \tag{16}$$

with

$$\mathbb{A} \triangleq \begin{bmatrix} \mathbb{O}_{3\times3} & \mathbb{I}_{3\times3} \\ g\,\mathbb{H} & -2\,\mathbb{E} \end{bmatrix} \quad , \quad \mathbb{H} = \begin{bmatrix} h_{11} & h_{12} & h_{13} \\ h_{21} & h_{22} & h_{23} \\ h_{31} & h_{32} & h_{33} \end{bmatrix} \quad , \quad \mathbb{E} = \begin{bmatrix} 0 & -1 & 0 \\ 1 & 0 & 0 \\ 0 & 0 & 0 \end{bmatrix} \tag{17}$$

where $\mathbb{O}$ and $\mathbb{I}$ are the zero and identity matrices, respectively, and h_{ij} is the generic component of the second order tensor $\boldsymbol{H}$ in the RTN reference frame. Equation (16) represents a system of first-order differential equation with periodic coefficients (of period 2π), and its stability analysis may be performed (numerically) with Floquet's theory [8].

Numerical simulations show that stable AEPs exist in the plane of motion of the two attractors. For instance, Figure 3 shows examples of those stability regions in the neighborhood of the classical Lagrange points L_1 and L_4 in the Sun-[Earth+Moon] system. In particular, the stability regions are not uniform due to the presence of instability stripes caused by the eccentricity of the Earth's orbit around the Sun. These instability stripes are consistent to those found in Ref. [2] in the special case of radial propulsive acceleration . In fact, when $\alpha = 0^\circ$ Fig. 3(a) shows the instability of the so called L_1-type AEPs (that is, AEPs placed along the segment between the Sun and L_1 point), while Fig. 3(b) reveals the existence of stable triangular points (that is, located on a circle of unit radius and centered at the Planet).

Conclusions

The existence and stability of AEPs for an E-Sail based spacecraft have been investigated within an elliptical restricted three-body problem under the assumption of constant orientation of the E-sail nominal plane. The equilibrium points belong to the plane on which the two primaries move and consist of segments along which the spacecraft oscillates back and forth synchronously to the motion of the Planet. The linear stability analysis for the Sun-[Earth+Moon] system has shown the existence of stable regions of AEPs close to the classical equilibrium points L_1 and L_4.

The propulsive acceleration required to generate AEPs in the neighborhood of the L_1 point in the Sun-[Earth+Moon] system are compatible with the capabilities of a first order generation E-Sail propulsion system. In fact, the amount of propulsive acceleration fluctuation depending on the true anomaly of the Planet is moderate and may be compensated through a suitable variation of the E-sail tethers' voltage.

Acknowledgements

This research was financed in part within the European Community's Seventh Framework Programme ([FP7/2007-2013]) under grant agreement number 262733.

References

[1] McKay, R. J., Macdonald, M., Biggs, J., and McInnes, C., "Survey of Highly-Non-Keplerian Orbits with Low-Thrust Propulsion," *Journal of Guidance, Control, and Dynamics*, Vol. 34, No. 3, May-June 2011, pp. 645–666. doi: 10.2514/1.52133.

[2] Aliasi, G., Mengali, G., and Quarta, A. A., "Artificial equilibrium points for a generalized sail in the elliptic restricted three-body problem," *Celestial Mechanics and Dynamical Astronomy*, Vol. 114, No. 1-2, October 2012, pp. 181–200. doi: 10.1007/s10569-012-9425-z.

[3] Janhunen, P. and Sandroos, A., "Simulation study of solar wind push on a charged wire: basis of solar wind electric sail propulsion," *Annales Geophysicae*, Vol. 25, No. 3, March 2007, pp. 755–767. doi: 10.5194/angeo-25-755-2007.

[4] Baoyin, H. and McInnes, C. R., "Solar Sail Equilibria in the Elliptical Restricted Three-Body Problem." *Journal of Guidance, Control, and Dynamics*, Vol. 29, No. 3, May-June 2006, pp. 538–543. doi: 10.2514/1.15596.

[5] Szebehely, V., *Theory of orbits: the restricted problem of three bodies*, Academic Press, New York, 1967, pp. 587–602.

[6] Janhunen, P., Toivanen, P. K., Polkko, J., Merikallio, S., Salminen, P., Haeggström, E., Seppänen, H., Kurppa, R., Ukkonen, J., Kiprich, S., Thornell, G., Kratz, H., Richter, L., Krömer, O., Rosta, R., Noorma, M., Envall, J., Lätt, S., Mengali, G., Quarta, A. A., Koivisto, H., Tarvainen, O., Kalvas, T., Kauppinen, J., Nuottajärvi, A., and Obraztsov, A., "Electric solar wind sail: Toward test missions," *Review of Scientific Instruments*, Vol. 81, No. 11, November 2010, pp. 111301–1–11301–11. doi: 10.1063/1.3514548.

[7] Mengali, G., Quarta, A. A., and Janhunen, P., "Electric sail performance analysis," *Journal of Spacecraft and Rockets*, Vol. 45, No. 1, January-February 2008, pp. 122–129. doi: 10.2514/1.31769.

[8] Hale, J. K., *Ordinary Differential Equations*, Dover Publications, Inc., New York, 1980, pp. 117–121, 280, ISBN: 0-486-47211-6.

List of Figures

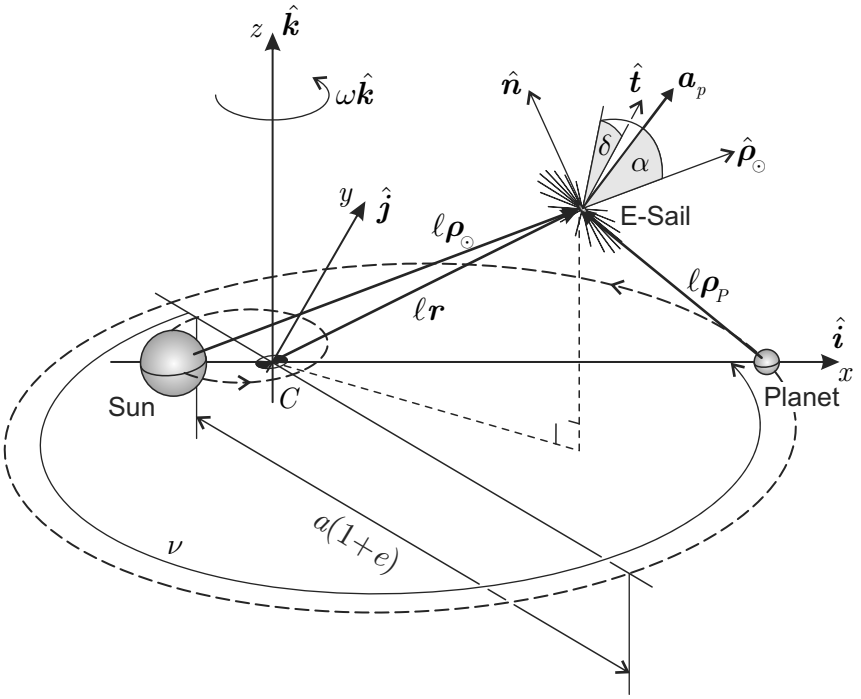

Figure 1: E-Sail in the elliptical restricted three-body problem.

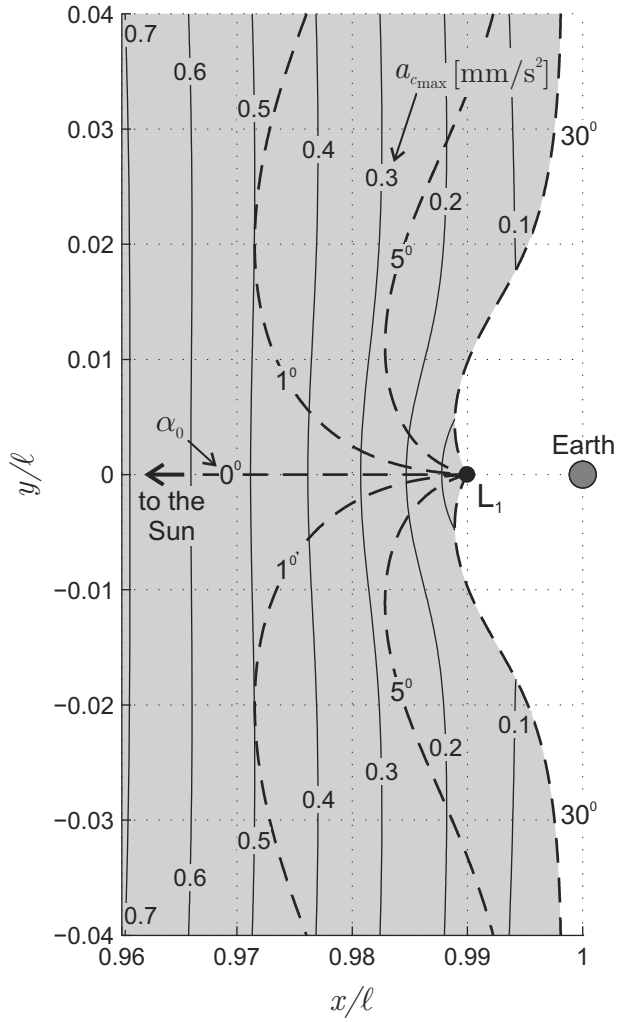

Figure 2: E-Sail performance for AEPs close to L_1 in the Sun-[Earth+Moon] system, with $\delta_0 = 0°$ when $y/\ell > 0$ and $\delta_0 = 180°$ when $y/\ell < 0$.

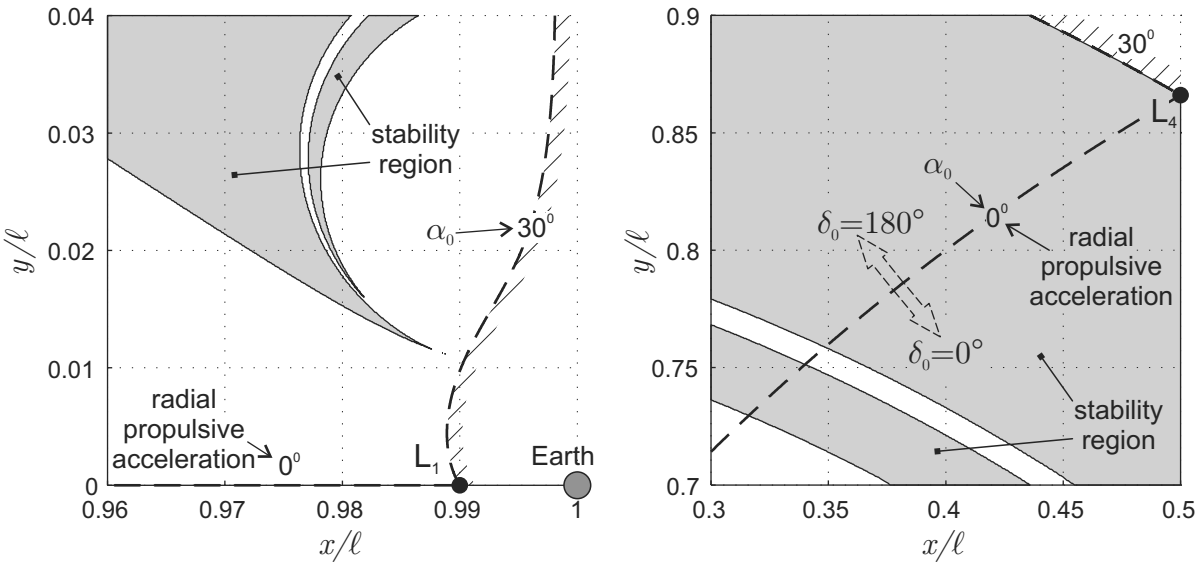

a) Stability region close to L_1 with $\delta_0 = 0°$.

b) Stability region close to L_4.

Figure 3: Stability regions close to the classical equilibrium points L_1 and L_4 in the Sun-[Earth+Moon] system.